Product User Guide (PUG)

glaciers cci

Prepared by: Glaciers_cci consortium
Contract: 4000109873/14/I-NB
Name: Glaciers_cci-D3.3_PUG
Version: 1.6
Date: 05.10. 2017

Contact:
Frank Paul
Department of Geography
University of Zurich
frank.paul@geo.uzh.ch

Technical Officer:
Stephen Plummer
ESA ESRIN

Document status sheet

Version	Date	Changes	Approval
0.1	22.05. 2013	Initial draft	
0.2	24.05. 2013	Draft with example glacier area	
0.3	24.10. 2013	Velocity and DEM differencing integrated	
0.4	13.11. 2013	Altimetry added and area finalized	
0.5	13.03. 2013	Comments of the TO integrated	
0.6	13.06. 2013	Final consortium feedback integrated	
0.7	06.08. 2014	Reply from consortium to TO comments integrated	
1.1	04.04 2015	Update of year 1 in Phase 2	
1.2	15.05. 2015	Consortium feedback integrated	
1.3	16.06. 2015	Feedback from TO integrated	
1.4	22.02. 2016	First update of year 2 in Phase 2 (Introduction)	
1.4	16.04. 2016	Consortium feedback integrated (Section 5.2)	
1.5	25.08. 2016	Comments from TO integrated	
1.5	25.10. 2016	Some final comments from TO integrated	
1.6	05.10. 2017		

The work described in this report was done under ESA contract 4000109873/14/I-NB. Responsibility for the contents resides with the authors that prepared it.

Author team:
Frank Paul (GIUZ), Robert McNabb, Christopher Nuth, Andreas Kääb (all at GUIO), Thomas Nagler, Gabriele Bippus, Jan Wuite (all at ENVEO), Kate Briggs, Andrew Shepherd (all at SEEL), Tazio Strozzi (Gamma)

Glaciers_cci Technical Officer at ESA:
Stephen Plummer

Table of Contents

Executive Summary **4**

1. Introduction **5**

2. Glacier area **6**

- **2.1 Product content** **6**
- **2.2 Product format** **7**
- **2.3 Known limitations** **9**
- **2.4 Available software tools and data access** **10**

3. Elevation change (altimetry) **11**

- **3.1 Product content** **11**
- **3.2 Product format** **13**
- **3.3 Known limitations** **15**
- **3.4 Available software tools** **16**

4. Elevation change (DEM differencing) **17**

- **4.1 Product content** **17**
- **4.2 Product format** **18**
- **4.3 Known limitations** **19**
- **4.4 Available software tools** **19**

5. Velocity (optical and microwave) **20**

- **5.1 Product content** **20**
- **5.2 Product format** **21**
- **5.3 Known limitations** **24**
- **5.4 Available software tools** **25**

References **26**

Abbreviations **28**

Executive Summary

This document is deliverable 3.3 of the Glaciers_cci project, the Product Users Guide (PUG). The PUG describes the FCDR and ECV data products on glacier area, surface elevation changes and ice velocity fields for users. This includes the detailed description of:

- the geophysical data product content
- the product flags and metadata
- the data format
- the product grid and geographic projection
- known limitations of the product
- available software tools for decoding and visualization of the data.

In the following we describe these details for each of the generated products in a generic and simplified way based on the generated datasets. As some of the datasets have already been extensively used by the community (e.g. the Randolph Glacier Inventory, RGI) we also describe differences to other existing datasets (GLIMS database) and those that will be made available on the Glaciers_cci webpage (the so-called Climate Research Data Package, CRDP). Ultimately, the glacier area product will be integrated in the GLIMS database and the elevation change information will be a part of the new WGMS database. Velocity fields are so far only stored on the project webpage and might find another long-term storage later on (e.g at the ENVEO cryoportal).

1. Introduction

The Glaciers_cci project has created a wealth of data for each of the three main products glacier area, elevation change and velocity. The primary product was the glacier area product that contributed to the globally near-complete glacier inventory that was prepared in support of IPCC AR5. This so-called Randolph Glacier Inventory (RGI) has already widely been used by the community and is provided in a data format, which is slightly different from the GLIMS format. The special RGI format was suggested by the user community and is thus well known to them. However, for those not familiar with it we describe the RGI format and its differences to the datasets stored in the GLIMS database also in this document. Further details about the RGI (e.g. the regional contributors) can be found in the technical documentation for RGI v5.0 by Arendt et al. (2015) and a freely available overview paper by Pfeffer et al. (2014). The datasets from the RGI have in the meantime been integrated into the GLIMS database. Due to the differing attribute data and the more generalized set-up of the RGI, proper integration was challenging. Once integrated, it is foreseen to supplement the RGI datasets in GLIMS automatically with further information (e.g. topogaphic attributes for individual glaciers).

Two further types of datasets were created in selected key regions: (a) those used in specific publications (e.g. on glacier elevation changes in Greenland and the greater Himalaya), and (b) those exclusively generated by Glaciers_cci as a response to the URD and recent needs of the science community (e.g. inventories for the Karakoram and Pamir region or velocity fields for Arctic Islands) but not yet published. These datasets are available in the dedicated CRDP database at Enveo via the Glaciers_cci webpage (link: ‘data access’). They will finally be integrated in the CCI data portal and the databases of the respective hosts (GLIMS, WGMS). As this is a still ongoing activity (e.g. Option 5 is working on integrating the elevation change data derived from remote sensing in the WGMS database) and subject to change, we focus for (a) and (b) on the description of the products as available from the CDRP of Glaciers_cci.

Further data products have been created in all three years of CCI Phase 2. They are consistent with what has been described in the Phase 1 document for the glacier area and velocity products, but further details have been added for velocity (e.g. example csv file and header information in xml format) to the year 2 update of the document. For the elevation change product described in Ch. 3 adjustments were applied to consider new datasets (e.g. Cryosat 2) and new information is provided to consider a new method of determination (altimetry trends vs a DEM reference surface). Some smaller issues have been added for the year 3 update of this document (e.g. data formats and access to Sentinel 2, and the synergystic use of velocity products from optical and SAR sensors).

2. Glacier area

2.1 Product content

The glacier area product is an outline marking the extent of a glacier that is physically defined as (Cogley et al., 2011): "*A perennial mass of ice, and possibly firn and snow, originating on the land surface by the recrystallization of snow or other forms of solid precipitation and showing evidence of past or present flow*." This vector line is indefinitely sharp, suggesting that also the boundary of a glacier is well defined. As the image of a typical glacier in the Alps in Fig. 2.1 reveals, this is not the case. Where the glacier is covered by debris (left side), the boundary is rather fuzzy and might even in the field be difficult to define. This local uncertainty changes from analyst to analyst (Paul et al., 2013) and is not reported with the outline. It is thus recommended to overlay the outlines in the CRDP (Glaciers_cci, 2015) with other datasets (e.g. high-resolution satellite imagery in Google Earth) before the product is used for other applications (e.g. change assessment).

Fig. 2.1: A typical glacier in the Alps (Oberaarglacier) showing bare and snow-covered ice, as well as debris cover on the surface and deposited on lateral moraines (Photo: F. Paul).

As glacier flow is not normally detectable on single satellite images, a further definition has been introduced for the purpose of GLIMS that is tailored to the remote sensing perspective (Raup and Khalsa, 2010): "*A glacier or perennial snow mass, identified by a single GLIMS glacier ID, consists of a body of ice and snow that is observed at the end of the melt season, or, in the case of tropical glaciers, after transient snow melts. This includes, at a minimum, all tributaries and connected feeders that contribute ice to the main glacier, plus all de-*

bris-covered parts of it. Excluded is all exposed ground, including nunataks." There are ten additional remarks on this definition to guide the analyst that are not repeated here, but used as a guide for the delineation of the Glaciers_cci area product.

In addition to the physical definition given above this remote sensing perspective also introduces a more conceptual viewpoint related to glacier tributaries. In the case two glaciers are in contact (without joint flow), they should be treated as individual entities. Handling this rule consistently for all glaciers is rather challenging, so the extent and shape of the glacier entity as defined by the ID of a polygon can vary with the analyst without being wrong. In this regard, there will be neither a unique and correct number for glacier counting nor for glacier size in a given region. This also applies to the outlines in the CRDP. In Fig. 2.2 we show an example of the outlines for the glacier depicted in Fig. 2.1 and the surrounding region (see Fig. 2.3 for an overlay with satellite image).

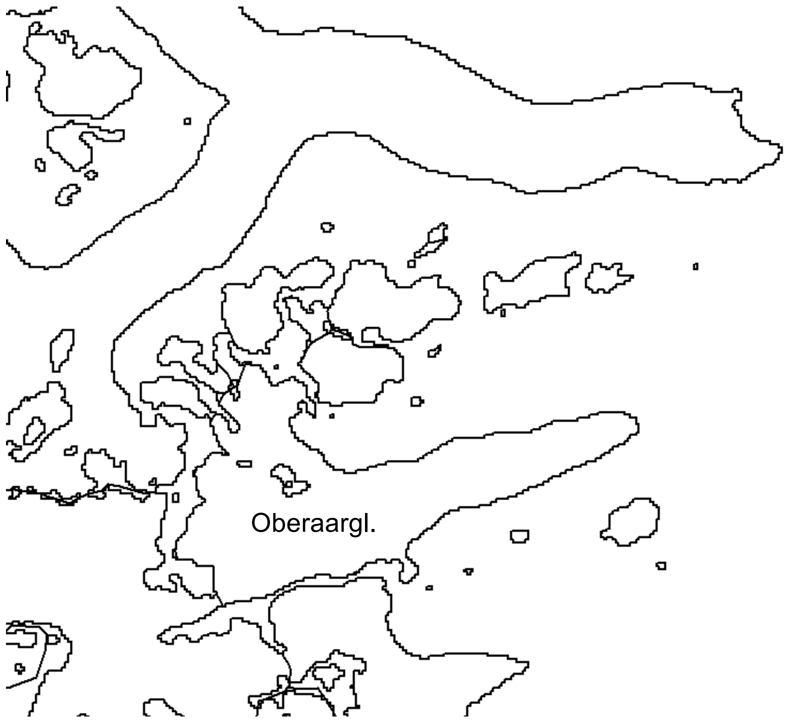

Fig. 2.2: Corrected glacier outlines (debris and drainage divides added, lakes removed).

2.2 Product format

There are three principle outlets for the generated glacier area products: (1) the GLIMS database, (2) the Randolph Glacier Inventory (RGI) and (3) the Glaciers_cci website (providing a link to the CRDP). These datasets differ in regard to map projection, appended meta-information, file format, and others. Also file names are not fixed and partly depend on the data source. In Table 2.1 we provide an overview on some key characteristics of the different formats. The mentioned Table 3.1 in the PSD (Glaciers_cci, 2011b) provides more detailed information on the individual files of the GLIMS format. Depending on the foreseen application, one or the other dataset might be more appropriate for the respective users. At a later stage all datasets will also be available in the GLIMS database.

	GLIMS database	RGI@GLIMS	Glaciers_cci
Projection	geographic	geographic	UTM
Datum	WGS84	WGS84	WGS84
Meta-information	full according to GLIMS specification	reduced (only basic data)	internal (not GLIMS compliant but with topographic attributes)
Files	4 individual shape files (see Table 3.1 in PSD)	1 shapefile	1 shapefile
Accuracy	best possible	partly preliminary	best possible
Purpose	long-term archive, multi-temporal datasets	Global-scale appli-cations for IPCC	documentation of generated datasets (finally be in GLIMS)
Time-stamp	yes	partly yes	yes
Satellite scene?	quicklook-footprint	no	quicklooks
Format	shp, kmz, and others	shp	shp and grids (on request)
Download	numerous options, map-based selection	ftp site	website

Table 2.1: Key characteristics of the glacier area product in the different databases.

2.2.1 The format of the RGI datasets

Many of the datasets produced by Glaciers_cci were provided to the RGI in a plain shapefile format (available in the CRDP, see 2.2.2) and were transformed collectively into the RGI format by the RGI team. As this format is different from the GLIMS format, we provide in Table 2.2 the details of the RGI attribute table. The files are sorted for 19 key regions and can be downloaded all at once or per region from glims.org/RGI.

Attribute	Format	Content
RGIId	character	Identifier (unique within the RGI)
GLIMSId	character	Identifier (GLIMS format)
RGIFlag	character	Qualifiers of glacier eligibility
BgnDate	YYYYMMDD	Date of outline, or first date of a range
EndDate	YYYYMMDD	End date of a range
CenLon	numeric	Longitude of glacier centroid (deg)
CenLat	numeric	Latitude of glacier centroid (deg)
O1Region	numeric	First-order region number (Table S1)
O2Region	numeric	Second-order region number (Table S1)
Area	numeric	Area of glacier (km^2)
Type	character	Terminus-type code
Name	character	Name of glacier

Table 2.2: Attribute information for the glaciers in the RGI.

2.2.2 The format of the Glaciers_cci datasets

The glacier outlines are also available from the CRDP website (http://glaciers-cci.enveo.at). The data files contain a varying degree of attribute information within each shapefile (e.g. a GLIMS-ID and/or topographic attributes) and are accompanied by meta-information compiled in a separate file that can be downloaded by clicking on the 'i' (information) letter. The information includes (among others): Entry ID, summary description, data set citation / reference / creator / title / project / date / version / institution, geographic coverage and extent (coordinates), projetion and platform information (e.g. sensor, path, row, date range), processing method, format, file size and review dates. Examples of such metadata information sheets are provided in the Annex of the CRDP (Glaciers_cci, 2015).

2.3 Known limitations

Glacier outlines are very dependent on manual interpretation. This can be done either with support of the automated classification of clean ice or not, but each glacier has to pass the critical review of the analyst and is corrected against reference datasets as required and as available. For example, unmapped debris has to be added and wrongly mapped lakes need to be removed as illustrated in Fig. 2.3. The final product only includes the corrected glacier extents, i.e. the outer yellow and red outlines. Due to the required manual intervention and the regionally sometimes challenging mapping conditions (e.g. debris identification), product accuracy is variable. This is in general not visible on a glacier-by-glacier basis from the accuracy information stored in the meta-data, as the given values refer to mean values over the entire region or satellite scene. Known regions with maybe reduced accuracy are found where a glacier is covered by debris or located in shadow, where optically thin clouds (fog, haze, cirrus) cover a scene, where the terminus is in contact to water (that might be turbid or have sea ice or ice bergs on it), and where seasonal snow and optically thick clouds cover a scene. For users of the glacier outlines it is thus most important to roughly check them (e.g. by overlaying them in Google Earth or similar tools) before using them for a specific purpose, as our interpretation of outlines might be different than those required for a specific application.

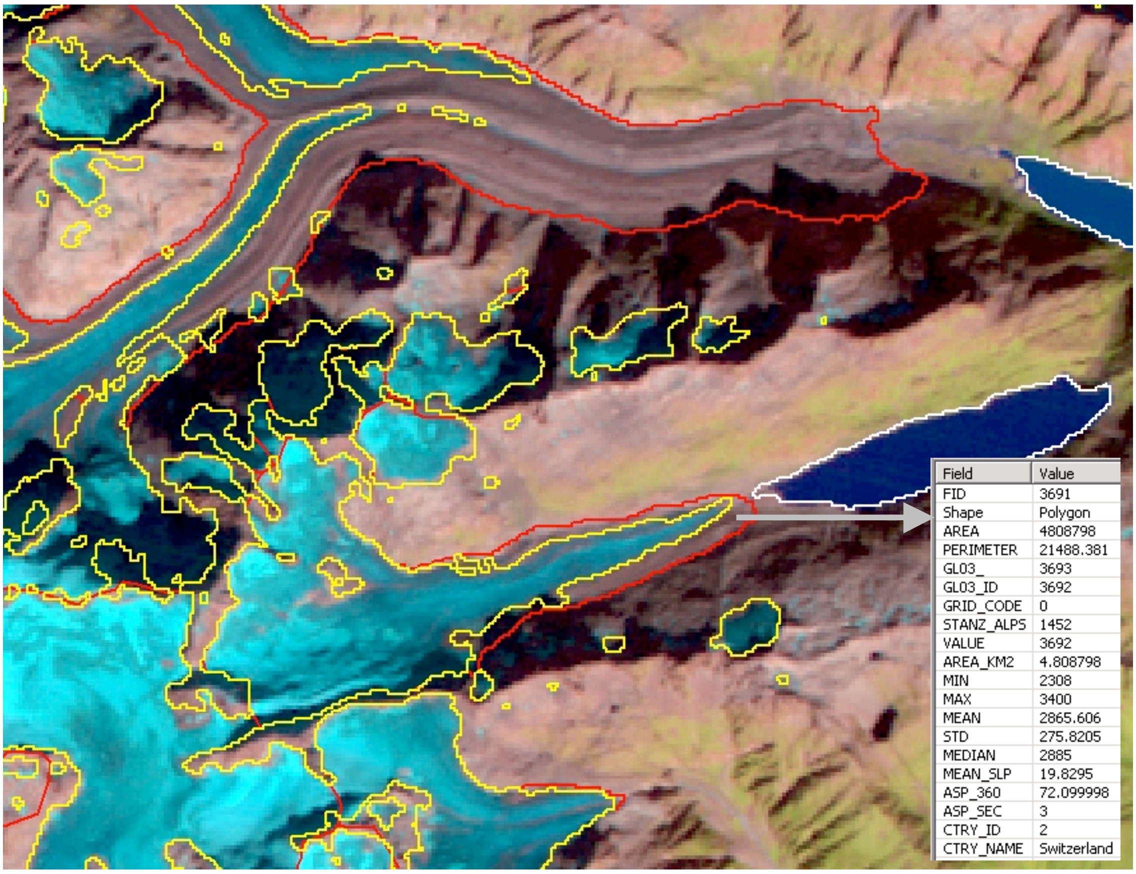

Fig. 2.3: Glacier outlines from 2003 as derived from the band ratio (yellow). The analyst has to add debris cover (red) and remove lakes (white). The final outlines are composed of the outer yellow and red lines (cf. Fig. 2.2). The satellite image in the background is from 2009. The meta-information available in the attribute table for Oberaarglacier is shown in the inset.

The latter implies that two different interpretations of a glacier outline can both be correct for a specific purpose. So any measure of uncertainty should focus on the variability in interpretation by the same operator. Based on the results of the study by Paul et al. (2013), we recommend performing a multiple digitization experiment whenever manual corrections are applied to glacier outlines to obtain at least an internal measure of operator uncertainty. As this might not always be possible, results from the Paul et al. (2013) study should be adopted to the extent possible and reported. A series of further measures can be applied to report product uncertainty such as the buffer method for clean ice, but these have their own limitations (for details see Glaciers_cci, 2016). In effect, uncertainty measures will in general neither be provided per pixel (as for velocity) nor per glacier (as for elevation change), but as a mean value for the entire analysed sample based on a few selected examples. Apart from this, some words on snow, cloud and shadow conditions are also required as these govern completeness of the dataset and highlight if and where outlines have been interpolated (or taken from other sources). As an update in year 3 of phase 2 of Glaciers_cci, we have decided to provide uncertainty information (alpplied methods and results) directly in the metadata information sheet for each dataset in the CRDP.

2.4 Available software tools and data access

2.4.1 Software tools

Glacier outlines are produced in a vector format (ESRI shape file) from orthorectified satellite images, predominately Landsat 5, 7 and 8 data that are available as Geotif files and Sentinel 2 data available in jpeg2000 format. The former two formats can be opened, analysed and changed with public domain image viewers (e.g. xv, ImageMagick) and GIS software (e.g. QGIS), but commercial software packages (e.g. ENVI or ESRI products) are also widely applied. The jpeg2000 format is correctly imported by QGIS and ArcMap from ESRI. As the ESRI shapefile format is open, it can be converted to all other formats, including kmz (for overlay in Google) or grid (raster) formats at the required spatial resolution. The meta-information stored in the attribute tables can be exported to other text (e.g. csv) or database (e.g. dbf) formats and thus easily processed outside the GIS. The screenshot in Fig. 2.3 shows how the glacier outlines and the meta-information for one glacier look like in ArcGIS.

2.4.2 Data access

The data created by the Glaciers_cci project can be downloaded in geographic projection with WGS84 datum from the GLIMS database (full inventory information in GLIMS format) at glims.org or the RGI (with reduced meta-data in RGI format) at glims.org/RGI. The created shapefiles are also available in their original format from the CDRP website at: http://glaciers-cci.enveo.at using UTM projection with WGS84 datum. The original images from the Landsat satellite series are freely available in Geotif format from glovis.usgs.gov. Sentinel 2 scenes can be downloaded from the Sentinel science hub (scihub.copernicus.eu) as well as glovis.usgs.gov. It is currently also possible to access a cloud service from Amazon via remotepixel.ca (Landsat 8 and Sentinel 2 only). The generated outlines are shown for all regions along with a list of the satellite scenes used in the CRDP technical document (Glaciers_cci, 2013b).

3. Elevation change (altimetry)

3.1 Product content

Elevation change estimates for large ice caps are generated for the period 2002 to 2014 from ICESat, EnviSat and CryoSat-2 using a repeat track plane fitting approach (e.g. Moholdt et al., 2010; McMillan et al., 2014). The general methods used, the product format, known limitations of the data, and available software tools that may be used to display and further maniupulate the data are outlined in this Section.

We use ICESat data from the ICESat GLAH06 dataset. This dataset is already corrected for most geophysical and instrumental effects however, we additionally apply corrections for sensor saturation and inter-campaign bias effects. The saturation correction was applied as recommended in the GLAH06 data dictionary, at
http://www.nsidc.org/data/docs/daac/glas_altimetry/data-dictionary-glah06.html and the inter-campaign bias effect was corrected as described by Borsa et al. (2013). The data are filtered to remove:

- all data flagged as 'elevation unusable' in GLAH06,
- all data without a valid saturation correction where one is needed,
- all data from poor quality campaign 2C, as per Smith et al. (2009),
- all data that is not part of a glacier, and
- residuals of greater than 5 m from the iterative plane fit.

The glacier filtering uses the RGI shapefiles to determine the surface type at the measurement location. The plots in Fig. 3.1 illustrate the data and results available from ICESat repeat track analysis over the Larsen C ice shelf and the Antarctic Peninsula. The images clearly reveal how the much steeper terrain of the latter region (that is typical for glaciers) strongly reduces the number of useable observations.

The initial Envisat dataset comes from Envisat L2 GDR_v2.1 data. The elevation measurements used are from the ice1 range measurement, with dry and wet tropospheric, ionospheric, tidal loading, and solid Earth tide corrections applied
(https://earth.esa.int/pub/ESA_DOC/ENVISAT/RA2-MWR/PH_light_1rev4_ESA.pdf).
Only datapoints flagged as high quality by the ice1 retracking quality flag are accepted and all points not falling on ice (as described for ICESat above) are removed.

Ice sheet elevation is calculated from CryoSat-2 SARIn mode data as the difference between satellite locations and range measurements corrected for the lag of the leading edge tracker [Wingham et al., 2006], fluctuations in dry and wet atmospheric mass, the effects of the ionosphere, and for solid Earth and ocean tides. We remove all datapoints where the interferometer fails to compute an across track location and all points not falling on ice.

To compute elevation change, elevation measurements from the ICESat mission are collected into 'segments', each covering approximately 750 m by 350 m and centred along the ground track. We fit an inclination- and time-variant plane to each segment with the time-variant coefficient of the model fit corresponding to the elevation change rate. For the EnviSat and CryoSat-2 data elevation measurements are collected into 1.2 x 1.2 km and 2 x 2 km 'tiles' respectively, and a plane is fitted to each tile. However, the greater spread of datapoints in the EnviSat and CryoSat-2 datasets allows a quadratic surface fit, which rises or falls linearly with time to give the elevation change rate. Backscatter corrections based on the backscattered power and local covariance of elevation (McMillan et al., 2014) are applied to the EnviSat and CryoSat measurements to remove the impact of temporal fluctuations in backscatter. We additionally remove all poorly constrained elevation change measurements from each dataset.

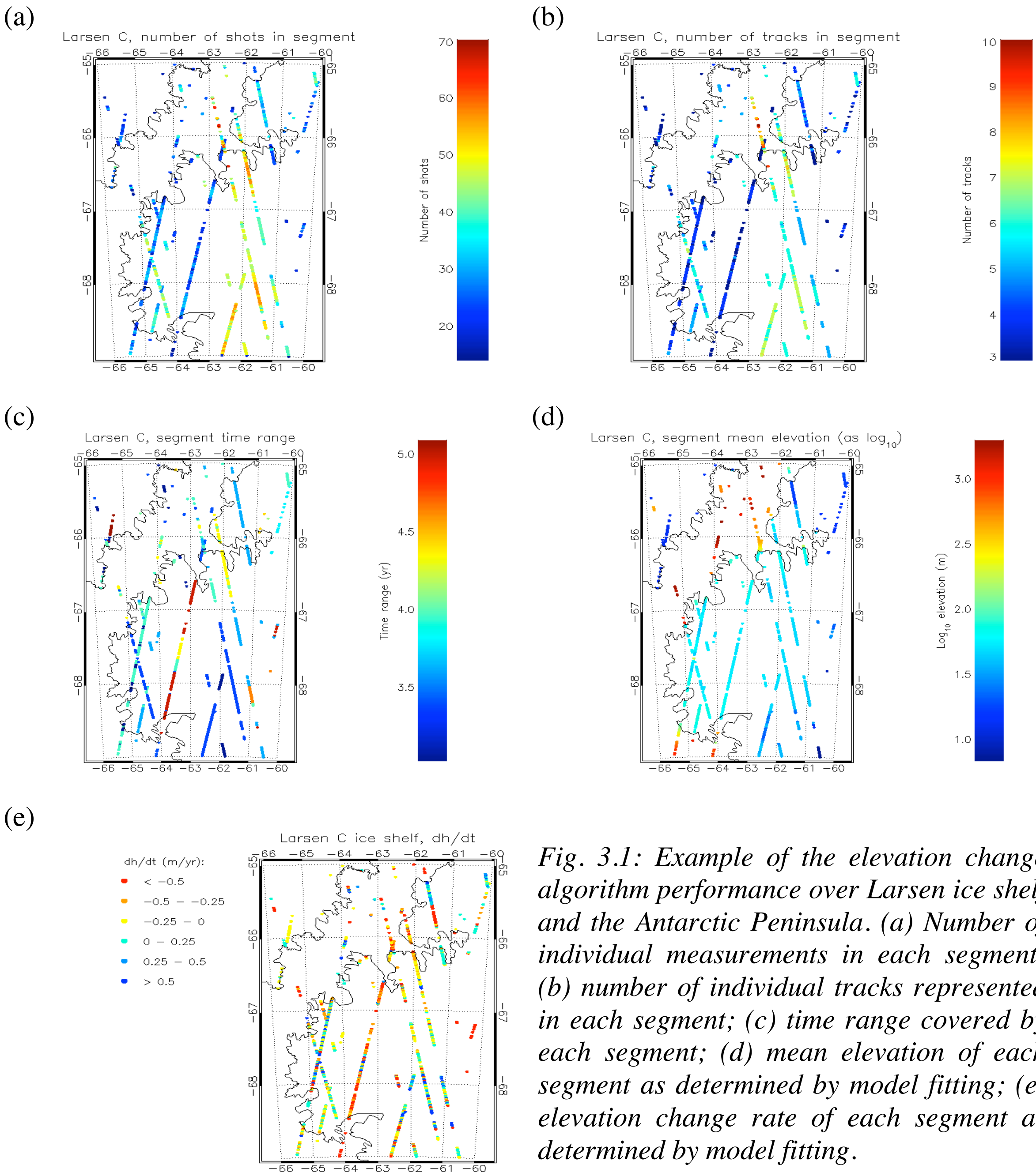

Fig. 3.1: Example of the elevation change algorithm performance over Larsen ice shelf and the Antarctic Peninsula. (a) Number of individual measurements in each segment; (b) number of individual tracks represented in each segment; (c) time range covered by each segment; (d) mean elevation of each segment as determined by model fitting; (e) elevation change rate of each segment as determined by model fitting.

Estimating glacier elevation change from ICESat altimetry in mountainous glacier regions involves the comparison to full coverage Digital Elevation Models (DEMs), such as from the Shuttle Radar Topography Mission (SRTM) of February 2000. ICESat GLA14 (release 531) datasets are extracted for all regions with glaciers including a 10 km buffer around glaciers for inclusion of stable terrain (Fig. 3.2). The SRTM geoid elevations are extracted to each ICESat footprint through bilinear interpolation, converted from the EGM96 to EGM2008 datum if necessary, and subsequently co-registered to all 17 ICESat campaigns. Band-ratios from a collection of Landsat images acquired around the year 2000 are used to generate a mask of off-glacier, clean ice, debris-covered ice, water and snow/firn.

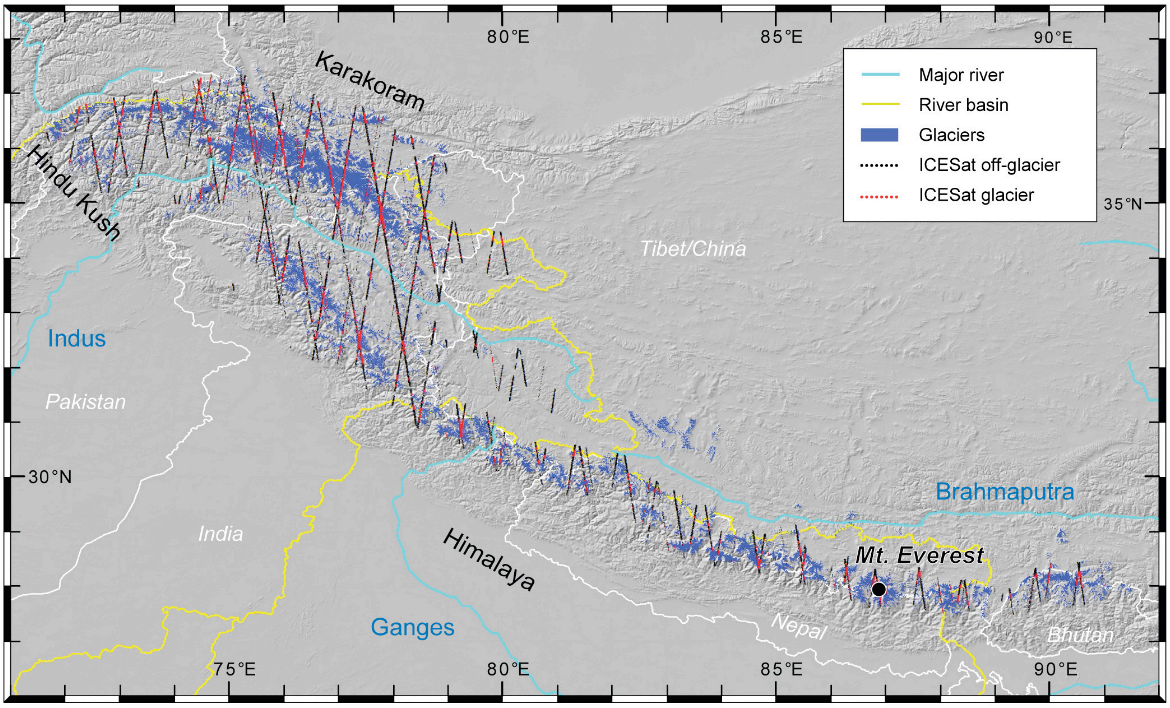

Fig 3.2 ICESat GLA14 (Release 531) over the Greater Himalaya Region showing off/on glacier footprints.

3.2 Product format

The product consists of a metadata file and a data file for each region investigated.

3.2.1 File naming convention

The convention for a metadata file is
ECA_NNNN_XXXXXN_YYYYYE_MM_YYMMDDS_YYMMDDE_SSmeta.csv
and the convention for a data file is
ECA_NNNN_XXXXXN_YYYYYE_MM_YYMMDDS_YYMMDDE_SS.csv, where:

- ECA indicates that this is an elevation change product
- NNNN indicates the geographic region
- XXXXXN is the latitude expressed in decimal degrees, XX.XXX, where N is the character that will be ‘N’ for ‘north’ or ‘S’ for ‘south’

- YYYYYE is the longitude expressed in decimal degrees, YY.YYY, where E is the character that will be 'E' for 'east' or 'W' for 'west'
- MM indicates the method – 'RT' indicates repeat track analysis
- YYMMDDS is the start date in YYMMDD
- YYMMDDE is the end data in YYMMDD
- SS indicates the sensor used
- .csv is the standard file extension for a comma-separated variable file

3.2.2 Metadata

The metadata for a given region is held in one comma-separated variable file. The entries for the crossover product are given in Table 3.1. Meta-information that is not applicable to the repeat track analysis is left blank – see the comments column for details.

Code	Name	Units	Comments
ECA1	Dataset link	alpha-numeric	Link to the related dataset (file name)
ECA2	Elevation source	alpha-numeric	Platform and sensor code
ECA3	Elevation URL	alpha-numeric	URL of data source
ECA4	Elevation notes	alpha-numeric	e.g. release number
ECA5	Cycles	numeric; 5 digits	Number of repeat cycles
ECA6	Cycles used	alpha-numeric	List of cycles used
ECA7	Reference cycle	numeric; 3 digits	Not applicable – the analysis produces absolute figures for elevation change and change rate
ECA8	Track 1 & mode	alpha-numeric	Not applicable – many tracks go into this analysis.
ECA9	Track 2 & mode	alpha-numeric	Not applicable – many tracks go into this analysis.
ECA10	Date start	numeric; 8 digits	Start of acquisition YYYYMMDD
ECA11	Date end	numeric; 8 digits	End of acquisition YYYYMMDD
ECA12	Latitude	alpha-numeric	Latitude of the segment centre in decimal degrees and the character 'N' for 'north' or 'S' for 'south'
ECA13	Longitude	alpha-numeric	Longitude of the segment centre in decimal degrees and the character 'E' for 'east' or 'W' for 'west'
ECA14	Projection	alpha-numeric	Geographic or UTM with zone
ECA15	Region	alphabetic	Country and region
ECA16	Methods	alphabetic	Method used – in this case repeat track
ECA17	Additional data	alphabetic	e.g. glacier mask used
ECA18	Analyst name	alpha-numeric	Name of the person who prepared the data
ECA19	Info	alphabetic	URL of extended information or publication
ECA20	Remarks	alpha-numeric	Any information not included above

Table 3.1: Metadata as available for the crossover product.

3.2.3 Data

The data for a given region is held in one comma-separated variable file. The entries for the crossover product are given in Table 3.2, while that for the ALT-DEM product is provided in Table 3.3. Information that is not applicable to the repeat track analysis is left blank – see the comments column for details.

Name	Units	Comments
Point latitude	Decimal degrees	North (+) or south (-), 4 dp minimum
Point longitude	Decimal degrees	East (+) or west (-), 4 dp minimum
Elevation change	Floating point (m/yr)	Elevation change rate as determined by the model fitted
Elevation change accuracy	Floating point (m/yr)	Accuracy (1 standard deviation) of the elevation change rate

Table 3.2: Data available in the repeat track product.

Column	Name	Units	Comments
1	Longitude	decimal degrees	WGS84
2	Latitude	decimal degrees	WGS84
3	GLA14 ellipsoide elevation	metres	
4	Saturation range correction	metres	
5	Geoide height	metres	EGM2008
6	Saturation indicator		
7	Footprint acquisition time	decimal years	
8	Geoid conversion	metres	EGM1996-EGM2008
9	SRTM elevation	metres	EGM1996
10	SRTM void fill indicator [	code	1: raw SRTM, 2: void
11	Elevation difference ICESat-SRTM	metres	dh = column 3 - column 5 + column 8 - column 9
12	Footprint class	code	1: off-glacier, 2: clean ice, 3: debris-covered ice, 4: water, 5: snow/firn

Table 3.3: Data available for the Altimetry-DEM products.

3.3 Known limitations

The repeat track analysis method (for ALT-DEM see below) assumes a number of conditions that may not be true to a greater or lesser extent. These include:

1) It assumes that a flat, inclined planar surface is a good fit to the ground below each segment. This may be true over a large, low-lying glacier, but not necessarily so in rough, mountainous regions.
2) It assumes that a long-enough time-range is present in the data to model long-term trends. The method cannot be applied if the seasonal signal is not properly established.
3) It models the long-term elevation trend as constant and uni-directional.
4) [ICESat only] It assumes that data affected by clouds can be accurately rejected before the modelling is applied.
5) It can only be applied to segments/tiles where enough good measurements exist to provide a reasonable model fit. In practice, the data as a whole should cover at least three years, have at least three individual tracks in each repeating track and have at least three data points in each individual track.

In this case, the product always meets the requirements stated in point 5. The user should be aware that short-period (e.g. seasonal) fluctuations in the elevation trend are not addressed, only a long-term average is calculated. It is also recommended that this product be used only in regions of slowly changing elevation such as over large and flat ice caps and ice fields, rather than over complex terrain. Complex terrain has slopes greater than 5°.

Limitations for the ALT-DEM product overlap in parts with the above limitations for the repeat track analysis. Specifically,

1) Due to noise in the altimetry data and the underlying reference DEM, and due to lack of representativeness of single tracks for mountain glaciers, trends can only be extracted on a regional (mountain range) basis. See Kääb et al. (2012, 2015) for typical region sizes.
2) Annual variations are not statistically significant, and only trends over the entire data set period of ICESat (2003-2009) should be analysed.
3) The method assumes that clouds are sufficiently detected and removed
4) The method also assumes that glacier and off-glacier footprints are separated, i.e. depends on the quality of the glacier inventory or manual classification used.

3.4 Available software tools

The data are provided in the csv file format. This data format can be imported easily by any programming language and most software tools (e.g. ArcGIS, ENVI, ERDAS Imagine). The metadata files contain the required information about projection.

4. Elevation change (DEM differencing)

4.1 Product content

Elevation changes of glaciers are measurements of the changing geometry of the glacier through time. At single points on the glacier, they are the result of both meteorological processes such as ablation and accumulation and dynamic processes such as ice emergence and submergence. For DEM differencing, the precision of the DEMs combined with the magnitude of change experienced by the glaciers, dictates the number of years required between repeat DEMs to significantly detect glacier elevation changes. Commonly, a minimum of 5 years is required to accurately provide glacier elevation changes from DEM differencing, but this is of course dependent upon data and site conditions (Fig. 4.1). Elevation change obtained from two DEMs depends on the acquisition times and DEM differencing can not provide information other then the absolute vertical difference between exactly these acquisition times, for instance not about the variations of elevation change over the period covered.

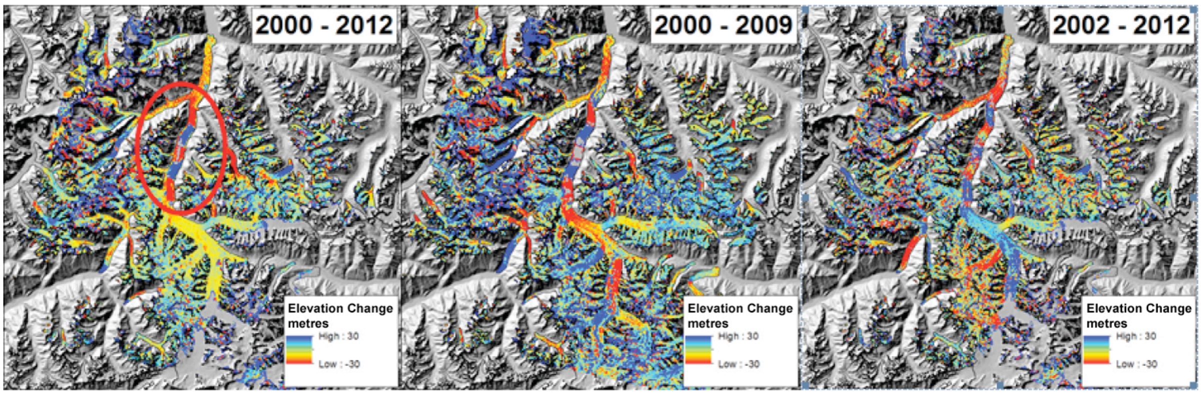

Fig 4.1: Example of the elevation change product (DEM differencing) in the Pamir region, Himalaya. The red circle shows a site- and data- specific artefact that occurs in all the optical ASTER stereo DEMs (see Section 4.3.2. known limitations). Only glacier changes are shown in the figure, though both glacier and off-glacier differences are provided in the final product.

The elevation difference product provided by DEM differencing is derived by a simple matrix subtraction between DEMs acquired with a multi-annual temporal separation. A number of processing steps are performed before the matrix subtraction. These include co-registration of the DEMs using the off-glacier terrain as a constraint (Nuth and Kääb, 2011). Further, if the two DEMs have different resolutions, then the highest resolution DEM is resampled to the lower resolution DEM. The resampling technique in general is bilinear interpolation to obtain the same grid points, but is also dependent upon the pixel size difference between the DEMs. If one pixel size is at least twice the second pixel size, then a moving block averaging is first applied to the highest resolution DEM. This is done to ensure that resolutions are as similar as possible before applying the bilinear interpolation to achieve an exact grid point match between the DEMs.

The quality of the elevation change product, as stated above, is dependent upon both the specific site and data being used. In some cases, the original DEMs from which to generate the elevation change product are provided with quality indicators (e.g. correlation values of optical-stereo DEMs). These are transferred through with the elevation change product to provide a quality mask(s) with the data. However, most globally available DEMs do not contain quality mask(s), and hence the elevation change products do not provide it as well.

The glacier elevation change product from DEM differencing provides the raw, unfiltered elevation changes for the entire area of interest (i.e. scene coverage). This includes both the changes on glaciers and the differences off-glacier. Therefore, the user, depending upon their use of the data, can estimate the accuracy of the changes. Using the differences off-glacier, error estimates may be computed based upon basic statistics such as mean, median, standard deviation and root mean square error (RMSE). A text header file provided with the data contains these statistics on stable terrain after the co-registration process (Fig. 4.2). Providing the full and raw DEM differences additionally gives the user a high flexibility in estimating the accuracy of the changes. This allows users, for example, to use glacier outlines other than the ones from RGI or Glaciers_cci or to apply higher order corrections such as for sensor jitter.

4.2 Product format

The DEM differencing elevation change product is provided as a geotif format in UTM projection. The naming convention includes the site name followed by the two specific dates of the DEM acquisitions used to generate the product. Quality masks (if available) are contained within the geotiff as an additional layer. A header file is currently included which describes the input data and some additional notes for use that are specific for each individual output product. These include statistics on stable terrain after co-registration within the Glaciers_cci processing system. An example header file is provided in Fig. 4.2.

```
Difference DEMs provided as a part of the ESA Glaciers_CCI project.

DEM1 source:                ASTER
DEM1 date:                  16.08.2012
DEM2 source:                ASTER
DEM2 date:                  11.02.2002
Region:                     Pamir
Pre-Processing:             Co-Registration
Remaining Errors(known):    1) ASTER Jitter; 2) SRTM snow/ice penetration
General Vertical Precision: 15 m
General Vertical Accuracy:  10 m
Analyst name:               Christopher Nuth

Specific Info
- DEM2 co-registered to DEM1. Linear translation of x, y and z are -15.05, -9.75 and -12.78 m, applied to DEM1.
- STABLE TERRAIN STATISTICS AFTER COREGISTRATION
                ALL stable terrain      Slope < 20 degrees
mean                    -2.85               -2.979
median                  -2.72               -2.819
standard deviation      20.19               17.999
RMSE                    20.369              18.22
number of samples       1851792             603989

Remarks
- These specific ASTER DEMs have problems/artifacts on the lower part of Fedchenko glacier which cause an
alternating (non-natural) positive/negative elevation change pattern. The artifacts are sensor and
site specific for this example. It is hypothesized that they result from the similarity of the glacier
contrast along this part of the glacier which runs in the same direction as the satellite overpass direction.

- The ASTER DEMs may contain along/cross track biases related to the precision of the satellite pointing
information and also from instrument shaking (jitter). This may lead to local biases of up to 10m.
See: Nuth and Kääb (2011). Co-registration and bias corrections of satellite elevation data sets for
quantifying glacier thickness change. The Cryosphere, 5, 271-290.
```

Figure 4.2: An example of the current DEM difference header file.

4.3 Known limitations

4.3.1 General issues

There are a number of known limitations that are specifically based upon the input data used as well as the environmental conditions at the site at the time of acquisition.

The elevation change produced from DEM differencing results in elevation changes covering the entire spatial domain of the glacier, in the most ideal situation, and for the period between acquisition dates of the DEMs. In many cases, there may be voids within the DEMs that consequently result in limited glacier coverage. This often occurs in optical stereo DEMs (e.g. ASTER, SPOT) at the upper reaches of the glacier where limited visual contrast hinders elevation extraction (see Fig. 4.1), or for example in interferometry (i.e. SRTM, TanDEM-X) from lack of phase coherence in the SAR image pair or from layover / foreshortening or mountain shadowing not visible to the side-looking sensor.

Interferommetric SAR DEMs (i.e. SRTM) may contain significant penetration on snow and ice, hence, the elevation surface may be below the actual glacier surface. Optical stereo data is dependent upon the visual contrast between images collected from different viewing angles. Thus, regions of low visible contrast (e.g. white surfaces in the accumulation areas of glaciers) may often result in voids, a very bumpy surface, or high residual errors. The user should consider whether these regions require removal before use of the data. Other potential in-scene biases include sensor specific biases. For example, ASTER DEMs may contain along/cross track biases related to the precision of the satellite pointing information and also from instrument shaking (jitter). This may lead to local biases of up to 10 m. Instrument vibrations are also a problem for the SRTM datasets.

4.3.2 Limitations of the provided datasets

For the provided datasets we identified the following limitations:

- The SRTM C-Band DEM contains significant penetration on snow and ice thus the surface of the SRTM DEM may be below the actual glacier surface.
- The ASTER DEMs have problems/artifacts on the lower part of Fedchenko glacier which cause an alternating (non-natural) positive/negative elevation change pattern (red circle in Fig. 4.1). The artifacts are sensor and site specific for this example. It is hypothesized that they result from the similarity of the glacier contrast along this part of the glacier which runs in the same direction as the satellite overpass direction.
- The ASTER DEMs may contain along/cross track biases related to the precision of the satellite pointing information and also from instrument shaking (jitter). This may lead to local biases of up to 10 m (see Nuth and Kääb, 2011).

4.4 Available software tools

All geospatial software (ArcGIS, ENVI, QGIS, GRASS) and most computational software (Matlab, Python, R) allow the import of geotif files. The geotif files contain metadata describing the geolocation, projection and pixel sampling of the data. And, as with all geotif files, the user is advised to take care that the header information is properly interpreted by the software used, in particular corner coordinates are not consistently imported.

5. Velocity (optical and microwave)

5.1 Product content

Glaciers move downhill due to the gravity-induced internal deformation of ice and through basal sliding. The rate of movement depends on many factors, including the underlying slope, the presence of liquid water on the bed, the climate, etc. The 3-dimensional flowpath of an ice particle through a body of ice is not accessible to remote sensing methods. Optical data are sensitive to surface features only, while the penetration depth of microwaves in dry snow and ice is in the order of a few metres to more than 100 m, depending on the radar frequency and snow and ice purity and structure (Ulaby et al., 1982; Mätzler, 1999; Rignot et al., 2001). While radar methods detect a mixture of surface and sub-surface features, it is generally referred to as "glacier surface flow" when derived from satellite measurements.

Velocity fields are estimated using optical or microwave repeat satellite data (Fig. 5.1). Block and feature matching techniques (e.g. the normalized cross-correlation; Kääb and Vollmer, 2000) are employed with both data sources. Before image matching, the two (or more) images have to be co-registered with subpixel accuracy. This can only be performed after accurate orthorectification for optical data and in the original sensor geometry for SAR data.

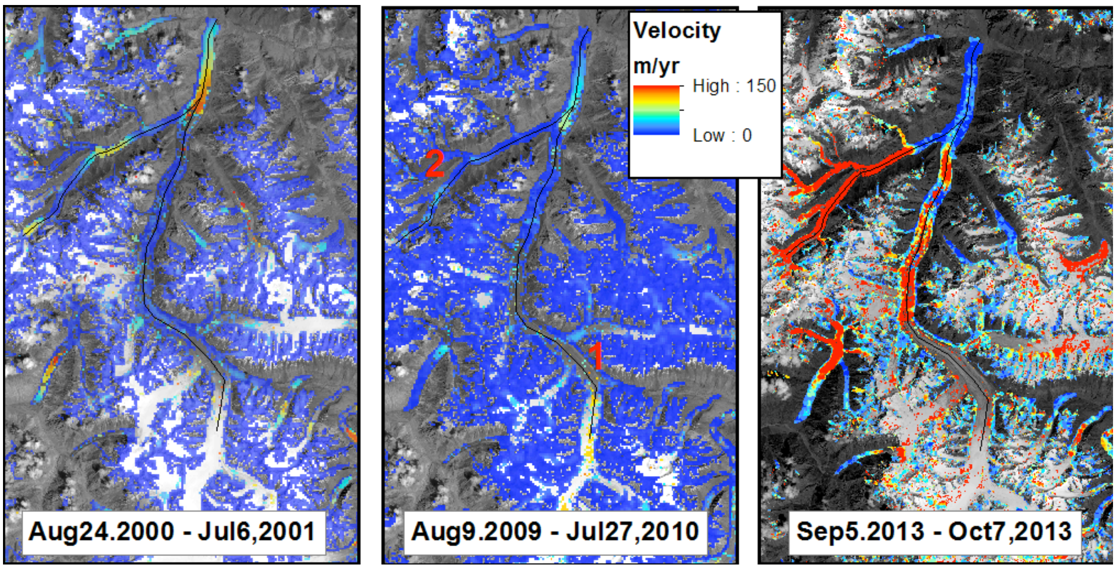

Fig. 5.1: Example of glacier displacement magnitudes from optical data for Fedchenko Glacier in the Pamir mountain range during three time epochs.

5.1.1 Products from optical sensors

The velocity product from optical images is based upon pre-orthorectified optical images that cover the same glacier(s) within a period of some months to several years. Image matching within an offset tracking procedure is then performed over the intersection of both optical image scenes, both on and off glacier. Off glacier offsets are used for co-registration and adjustment of the displacement field, or internal validation of the product. The output product is the raw co-registered displacements (unfiltered) for the area of interest (scene coverage).

5.1.2 Products from microwave sensors

The glacier velocity product from SAR data is commonly based upon images that cover the same glacier(s) within a period of some days to several weeks. Image matching within an off-set tracking procedure is performed over the intersection of both SAR image scenes, both on and off glacier, in the original radar geometry. Off-glacier offsets are used for co-registration and internal validation of the product. The native output products of SAR off-set-tracking procedures are co-registered displacements in the satellite line-of-sight and along track components for the entire area of interest (scene coverage). For final delivery and comparison with other products (e.g. from optical sensors), the raw satellite line-of-sight displacements are transformed to 2D horizontal velocity maps and orthorectified to a specific geographic projection.

5.2 Product format

The product format was defined according to the URD (Glaciers_cci, 2011a). The glacier velocity product from both optical and SAR images is provided as an ASCII file, e.g. csv format. This tabular file includes the X and Y coordinates, in a UTM projection, the displacement between the satellite images, the cross-correlation coefficient and signal to noise ratio as output from the image matching procedure, and then a mask code where 1 = glacier and 2 = non-glacier. The displacement measured between two optical images is given for successful matching locations, specified by Easting (X) and Northing (Y) coordinates of the local UTM zone, and the displacement in X and Y directions corresponding to displacements in Easting and Northing of the local UTM zone. An example of the optical velocity product as available in the CRDP document (Glaciers_cci, 2015) is provided in Figs. 5.2 and 5.3.

Pamir_optvel_09082009_27072010_colheaders.txt | Pamir_optvel_09082009_27072010.csv

```
Pamir_optvel_09082009_27072010.csv: Displacements between two panchromatic Landsat images
(Path/Row = 151/33) as described in:
Heid T. and Kääb A. Repeat optical satellite images reveal widespread and long term
decrease in land-terminating glacier speeds. The Cryosphere, 2012, 6, 467-478.

Col1 : X coordinate
Col2 : Y coordinate
Col3 : X-direction displacement (m)
Col4 : Y-direction displacement (m)
Col5 : Cross-correlation coefficient (NOTE: not normalized correlation coefficient).
Col6 : Signal-to-Noise Ratio
Col7 : MASK-  glacier == 1 , non-glacier == 2;

```

Fig. 5.2: Example of the optical velocity header.

Pamir_optvel_09082009_27072010_colheaders.txt | Pamir_optvel_09082009_27072010.csv

```
2.4566e+05,4.3914e+06,-100.39,-18.288,9.4397,2.6271,2
2.459e+05,4.3914e+06,62.817,-105.14,23.683,3.6793,2
2.4638e+05,4.3914e+06,-75.94,91.283,18.877,2.2573,2
2.4662e+05,4.3914e+06,-61.455,80.664,16.748,2.7558,2
2.4686e+05,4.3914e+06,69.639,87.152,21.93,2.6612,2
```

Fig. 5.3: Example of the optical velocity data set in csv format.

SAR images are given in two product formats. The main product format in Phase 1 of Glaciers_cci is provided in tabular format, given for each successful matching point (specified by Easting and Northing UTM coordinates or latitude and longitude coordinates) the derived displacement in line-of-sight direction of the radar beam (slant-range) and along track direction (azimuth direction). The naming convention includes the site name followed by the two specific dates of the satellite image acquisitions used to generate the product. A header file describes the input data and some additional comments that are specific for each individual output product, and the column headers for the csv file (see example in Fig. 5.4).

```
Pamir_mvvel_10012010_25022010_glims_id.csv: Displacements between two ALOS PALSAR images
(id: ALPSRP211170780 from 10.01.2010 and ic: ALPSRP217880780 from 25.02.2010)

Col1 (point_id):        id
Col3 (n_glims_id):      GLIMS ID
Col4 (n_parent_id):     Parent GLIMS ID (if exisitng)
Col5 (x):               X coordinate (UTM Zone 43N)
Col6 (y):               Y coordinate (UTM Zone 43N)
Col7 (vel_period):      3d-displacement (metres) for time between the image aquisitions
Col6 (vel_year):        3d-displacement (metres) yearly value extrapolated from the available period
```

Fig. 5.4: Header information of the SAR velocity data set in csv format.

The second product format is applied for Phase 2 of Glaciers_cci. The displacement from SAR data is given as a 2D horizontal velocity map (see Fig. 5.5), providing for each successful matching point the Easting and Northing velocity in m/day, which is the average velocity for the period of the two image acquisitions. The 2D magnitude (m / d) can be calculated as:

$$|v| = \sqrt{v_E^2 + v_N^2}$$

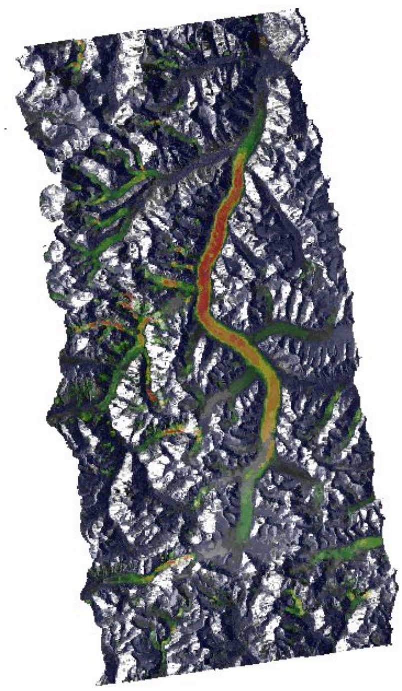

Fig. 5.5: Example map of the magnitude of ice velocity for Fedschenko glacier, Pamir, from TerraSAR-X.

The glacier velocity product is provided as an ASCII file (e.g. csv format) with the Easting and Northing coordinates (UTM or geographic projection), the elevation (optional), the Easting and Northing velocity in m/day, the height difference from the horizontal velocity field and the DEM (optional), and the cross-correlation coefficient or the signal to noise ratio as output from the image matching procedure (see example in Fig. 5.6). The displacement measured between two satellite images is given only for successful matching. Separate data files are distributed for each satellite image pair. The naming convention includes the Glaciers_cci products (IV, Ice Velocity), the RGI zone (e.g RGI09), and the dates and optionally times of satellite image acquisitions used to generate the product (e.g. 20100314T174956_20100429 T174933). A header file describes the input data and some additional comments that are specific for each individual output product, and the column headers for the csv file (see example below). In addition, a quick-look image of the product in jpg or tif format is provided.

398800	8136500	2.79838	0.0171509	0.03461557	-0.00000866	0.18406
398900	8136500	2.78028	0.01715156	0.03461538	0.00003564	0.18406
399300	8136500	3.3364	-0.00759969	0.04082833	-0.00010949	0.10131
399400	8136500	3.37779	0.00905482	0.04722597	-0.00023065	0.61946
398800	8136400	2.75372	0.03111035	0.03326074	0.00011377	0.30263
398900	8136400	2.95286	0.01715187	0.03461526	0.00012738	0.18406
399000	8136400	2.47543	0.04287975	0.07824819	0.00024021	0.26054
399100	8136400	2.71422	0.00477889	-0.02005771	-0.00001617	0.38003
399200	8136400	3.36793	0.00477999	-0.02005803	0.00013534	0.38003
399300	8136400	2.99533	-0.00760016	0.04082853	-0.000145	0.10131

Fig. 5.6: Example of the SAR velocity data set in csv format.

Example of the SAR velocity header in xml format:

```
<?xml version='1.0' encoding='utf-8'?>
<Velocity_Product>
  <MetadataFileVersion>
    <product>Ice Surface Velocity</product>
    <Version>V04</Version>
    <Date>2015-12-01</Date>
  </MetadataFileVersion>
  <link>
    <csvTableFilename>IV_RGI09_S1_20151004T030741_20151016T030741.csv</csvTableFilename>
    <csvTableFilename>IV_RGI09_S1_20151004T030741_20151016T030741.300.tif</csvTableFilename>
  </link>
  <processingInfo>
    <processingFacility>Gamma Remote Sensing</processingFacility>
    <processingSoftware>GAMMA Software</processingSoftware>
    <softwareVersion>4.7</softwareVersion>
    <processingDate>2015-12-10 17:20:15</processingDate>
    <method>Offset Tracking</method>
    <processingParameters>
      <filterWindowSize>
        <sizeX>512 pixels</sizeX>
        <sizeY>128 pixels</sizeY>
      </filterWindowSize>
      <oversamplingFactor>
        <SizeX>1</SizeX>
        <SizeY>1</SizeY>
      </oversamplingFactor>
    </processingParameters>
  </processingInfo>
  <productInfo>
    <productId>Ice Surface Velocity</productId>
    <productVersion>V01</productVersion>
    <productAlorithm>Offset Tracking</productAlorithm>
    <image1>2015 10 4 3 7 41.3083</image1>
    <image2>2015 10 16 3 7 41.4345</image2>
    <timeInterval>12.0000015 days</timeInterval>
```

```
    &lt;boundingBox&gt;
      &lt;northingUpperLeftCorner&gt;8168950.0000000&lt;/northingUpperLeftCorner&gt;
      &lt;eastingUpperLeftCorner&gt;329950.0000000&lt;/eastingUpperLeftCorner&gt;
      &lt;northingLowerRightCorner&gt;7980050.0000000&lt;/northingLowerRightCorner&gt;
      &lt;eastingLowerRightCorner&gt;562350.0000000&lt;/eastingLowerRightCorner&gt;
    &lt;/boundingBox&gt;
  &lt;/productInfo&gt;
  &lt;auxiliaryData&gt;
    &lt;auxiliaryData1&gt;TanDEM-X IDEM&lt;/auxiliaryData1&gt;
    &lt;auxiliaryData2&gt;RGI 5.0&lt;/auxiliaryData2&gt;
  &lt;/auxiliaryData&gt;
  &lt;inputSatelliteData1&gt;
    &lt;sensor&gt;>S1A IW IW1 HH&lt;/sensor&gt;
    &lt;acquisitionDate&gt;2015 10 4 3 7 41.3083&lt;/acquisitionDate&gt;
    &lt;acquisitionTime&gt;11275.2644700&lt;/acquisitionTime&gt;
    &lt;rangePixelSpacing&gt;2.3295620&lt;/rangePixelSpacing&gt;
    &lt;azimuthPixelSpacing&gt;13.8874000&lt;/azimuthPixelSpacing&gt;
    &lt;incidenceAngle&gt;33.3789000&lt;/incidenceAngle&gt;
    &lt;product&gt;SLC&lt;/product&gt;
  &lt;/inputSatelliteData1&gt;
  &lt;inputSatelliteData2&gt;
    &lt;sensor&gt;>S1A IW IW1 HH&lt;/sensor&gt;
    &lt;acquisitionDate&gt;2015 10 16 3 7 41.4345&lt;/acquisitionDate&gt;
    &lt;acquisitionTime&gt;11275.3906810&lt;/acquisitionTime&gt;
    &lt;rangePixelSpacing&gt;2.3295620&lt;/rangePixelSpacing&gt;
    &lt;azimuthPixelSpacing&gt;13.8873300&lt;/azimuthPixelSpacing&gt;
    &lt;incidenceAngle&gt;33.3770000&lt;/incidenceAngle&gt;
    &lt;product&gt;SLC&lt;/product&gt;
  &lt;/inputSatelliteData2&gt;
  &lt;CSVTableContents&gt;
    &lt;numberOfColumns&gt;7&lt;/numberOfColumns&gt;
    &lt;column1&gt;Northing (m)&lt;/column1&gt;
    &lt;column2&gt;Easting (m)&lt;/column2&gt;
    &lt;column3&gt;Elevation (m)&lt;/column3&gt;
    &lt;column4&gt;Velocity-x-Direction (m/day)&lt;/column4&gt;
    &lt;column5&gt;Velocity-y-Direction (m/day)&lt;/column5&gt;
    &lt;column6&gt;Velocity-z-Direction (m/day)&lt;/column6&gt;
    &lt;column7&gt;Cross-Correlation-Coefficient&lt;/column7&gt;
  &lt;/CSVTableContents&gt;
  &lt;mapProjection&gt;
    &lt;SRS&gt;["WGS 84 / UTM zone 40N", GEOGCS["WGS 84", DATUM["WGS_1984", SPHEROID["WGS 84",6378137,298.257223563, AUTHORITY["EPSG","7030"]], AUTHORITY["EPSG","6326"]], PRIMEM["Greenwich",0], UNIT["degree",0.0174532925199433], AUTHORITY["EPSG","4326"]], PROJECTION["Transverse_Mercator"], PARAMETER["latitude_of_origin",0], PARAMETER["central_meridian",57], PARAMETER["scale_factor",0.9996], PARAMETER["false_easting",500000], PARAMETER["false_northing",0], UNIT["metre",1, AUTHORITY["EPSG","9001"]], AUTHORITY["EPSG","32640"]]&lt;/SRS&gt;
  &lt;/mapProjection&gt;
  &lt;validation_QA-IV-2&gt;
    &lt;nrIcePoints&gt;12825&lt;/nrIcePoints&gt;
    &lt;nrValidPoints&gt;11126&lt;/nrValidPoints&gt;
    &lt;Percent&gt;86.7524&lt;/Percent&gt;
  &lt;/validation_QA-IV-2&gt;
  &lt;validation_QA-IV-3&gt;
    &lt;nrLandPoints&gt;620295&lt;/nrLandPoints&gt;
    &lt;mean&gt;0.0356901 (m/day)&lt;/mean&gt;
    &lt;stdev&gt;0.0416225 (m/day)&lt;/stdev&gt;
  &lt;/validation_QA-IV-3&gt;
  &lt;contactPerson&gt;
    &lt;Name&gt;Tazio Strozzi&lt;/Name&gt;
    &lt;email&gt;strozzi@gamma-rs.ch&lt;/email&gt;
    &lt;Affiliation&gt;Gamma Remote Sensing&lt;/Affiliation&gt;
  &lt;/contactPerson&gt;
&lt;/Velocity_Product&gt;
```

5.3 Known limitations

The accuracy of glacier velocity product from satellite images is dependent upon the scene resolution and quality as well as the absolute movement of the glacier between the scenes. This applies in general as well as for the datasets provided in the CRDP. Additional to the quality measures described in the UCR (Glaciers_cci, 2016) that are provided as additional datasets (e.g. correlation coefficient) and in the meta-data (e.g. displacement over stable terrain, error if reference data are available), the products that are distributed in the CRDP are going through a visual quality control (checking for geolocation, reasonable ice flow and remaining outliers) by the consortium (and science lead) and poor quality results are discarded or recalculated. However, the general issues mentioned below should be kept in mind by the final users for the interpretation of the products.

Known limitations for displacements from both optical and SAR data include:
- False matches: The match with the highest correlation coefficients might actually not represent the real glacier movement. Typical reasons for such false matches are features (such crevasses or ogives in optical images or speckle in radar images) that do not correspond but look similar in both images matched.
- Movement: The quality of matches does not depend in principle on the magnitude of glacier movement. However, large movements and, even more important, large movement gradients lead typically to strong changes and deformations of features so that matching accuracy drops or correct matches become impossible.

Known limitations for displacements specifically from repeat optical data:
- Cloud cover: Thin clouds that are transparent to some contrast features might allow for matching, but could also produce mis-matches. These effects can depend on the matching algorithm used (here normalized cross-correlation and orientation correlation).
- Contrast: Low visual contrast in the optical images prevents matching of features such as for optical stereo DEMs (see chapter on DEM differencing).

Known limitations for displacements specifically from repeat SAR data include:
- Wet snow-cover: The presence of wet snow-cover or ice on the surface of the glaciers changes dramatically the intensity of backscattering signal, precluding in most of the cases the successful use of matching algorithms.
- Large repeat-intervals: The longer the repeat interval between the two SAR images to be matched, the less correlation (e.g. speckle) between the backscattering signals, leading to less accurate results.
- Spatial resolution: High-resolution SAR sensors are preferred for monitoring the ice velocity especially of comparably small alpine glaciers. SAR sensors with lower spatial resolution generally lead to lower quality results and reduced spatial coverage of a glacier.
- Ionospheric artefacts: Ionospheric conditions during the acquisition of the images have an impact on the accuracy of the results, with stronger streaking effects at lower frequencies on the azimuth offset field.

Velocity products created from optical and SAR images can by used in synergy for glaciological investigations after adjustment to a common projection (e.g. Strozzi et al. 2017). Optical and SAR data are to a large extent complementary in the best timing of usage (SAR: Winter, optical: Summer). In addition, for past investigations or regular production, availability of redundant EO source data can guarantee a denser time series of results (e.g. Paul et al. 2017).

5.4 Available software tools

Most software packages are capable to import text-delimited files such as csv. Further, the csv can be converted to a shapefile for viewing the dataset in geospatial software (e.g. ArcGIS, GRASS, QGIS).

References

Arendt, A., et al. (2013): Randolph Glacier Inventory [v3.2]: A dataset of global glacier outlines. Global Land Ice Measurements from Space, Boulder Colorado, USA. Digital Media. (Online: http://glims.org/RGI/RGI_Tech_Report_V3.2.pdf)

Bolch, T., Sørensen, L., Mölg, N., Machguth, H., and Paul, F. (2013): Mass loss of Greenland's glaciers and ice caps 2003-2008 revealed from ICESat data. Geophysical Research Letters, 40, 875-881.

Borsa, A.A., Moholdt, G. Fricker, H.A. and Brunt, K.M. (2013): A range correction for ICESat and its potential impact on ice sheet mass balance studies. The Cryosphere, 7, 4287-4319.

Cogley, J.G., Hock, R., Rasmussen, L.A., Arendt, A.A., Bauder, A., Braithwaite, R.J., Jansson, P., Kaser, G., Möller, M., Nicholson, L. and Zemp, M. (2010): Glossary of Glacier Mass Balance and Related Terms. IHP-VII Technical Documents in Hydrology No. 86, IACS Contribution No. 2, UNESCO-IHP, Paris. 114 pp. (Online: http://unesdoc.unesco.org/images/0019/001925/192525E.pdf)

Glaciers_cci (2011a): User Requirements Document (URD). Prepared by the Glaciers_cci consortium, 45 pp.

Glaciers_cci (2011b): Product Specifications Document (PSD): Prepared by the Glaciers_cci consortium, 43 pp.

Glaciers_cci (2012): Product Validation and Algorithm Selection Report (PVASR): Prepared by the Glaciers_cci consortium, 113 pp.

Glaciers_cci (2015): Climate Data Research Package Technical Document (CRDP). Prepared by the Glaciers_cci consortium, 25 pp.

Glaciers_cci (2016): Uncrtainty Characterization Document (UCR). Prepared by the Glaciers_cci consortium, 34 pp.

Kääb, A. and M. Vollmer (2000): Surface geometry, thickness changes and flow fields on creeping mountain permafrost: automatic extraction by digital image analysis. Permafrost and Periglacial Processes, 11, 315-326.

Kääb, A.; Berthier, E.; Nuth, C.; Gardelle, J. and Arnaud, Y. (2012): Contrasting patterns of early twenty-first-century glacier mass change in the Himalayas. Nature, 488, 495-498.

Mätzler, C. (1999): Application of SMOS over terrestrial ice and snow, Proceedings of the 3rd SMOS Workshop, DLR, Oberpfaffenhofen, Germany, December 10-12.

Moholdt, G., Nuth, C., Hagen, J.O. and Kohler, J. (2010): Recent elevation changes of Svalbard glaciers derived from ICESat laser altimetry, Remote Sensing of Environment, 114, 2756-2767.

Nuth, C. and Kääb, A. (2011): Co-registration and bias corrections of satellite elevation data sets for quantifying glacier thickness change. The Cryosphere, 5, 271-290.

Paul, F., Barry, R., Cogley, J.G., Frey, H., Haeberli, W., Ohmura, A., Ommanney, S.J.S., Raup, B., Rivera, A. and Zemp, M. (2009): Recommendations for the compilation of glacier inventory data from digital sources. Annals of Glaciology, 50 (53), 119-126.

Paul, F., N. Barrand, E. Berthier, T. Bolch, K. Casey, H. Frey, S.P. Joshi, V. Konovalov, R. Le Bris, N. Mölg, G. Nosenko, C. Nuth, A. Pope, A. Racoviteanu, P. Rastner, B. Raup, K. Scharrer, S. Steffen and S. Winsvold (2013): On the accuracy of glacier outlines derived from remote sensing data. Annals of Glaciology, 54 (63), 171-182.

Paul, F., T. Strozzi, T. Schellenberger and A. Kääb (2017): The 2015 surge of Hispar Glacier in the Karakoram. Remote Sensing, 9(9), 888; doi: 10.3390/rs9090888.

Pfeffer, W.T., et al. (2014): The Randolph Glacier Inventory: a globally complete inventory of glaciers. Journal of Glaciology, 60 (221), 537-552.

Pritchard, H.D., Arthern, R.J., Vaughan, D.G., and Edwards, L.A. (2009): Extensive dynamic thinning on the margins of the Greenland and Antarctic ice sheets. Nature, 461, 971-975.

Raper, S.C.B. and Braithwaite, R.J. (2006): Low sea level rise projections from mountain glaciers and icecaps under global warming. Nature, 439, 311-313.

Raup, B. and Khalsa, S.J.S. (2007): GLIMS Analysis Tutorial, vers. 22/05/2007, Boulder, 15 pp. (Online: http://glims.org/MapsAndDocs/assets/GLIMS_Analysis_Tutorial_a4.pdf)

Rignot, E., Echelmeyer, K. and Krabill, W. (2001): Penetration depth of interferometric synthetic-aperture radar signals in snow and ice. Geophysical Research Letters, 28, 3501-3504.

Siegfried, M.R., Hawley, R.L. and Bikhart, J.F. (2011): High resolution ground-based GPS measurements show intercampaign bias in ICESat elevation data near summit, Greenland. Geoscience and Remote Sensing, 49(9), 3393-3400.

Smith, B.E., Fricker, H.A., Joughin, I.R. and Tulaczyk, S. (2009): An inventory of active subglacial lakes in Antarctica detected by ICESat (2003-2008). Journal of Glaciology, 55(192), 573- 595.

Strozzi T., A. Kääb and T. Schellenberger (2017): Frontal destabilization of Stonebreen, Edgeøya, Svalbard. The Cryosphere, 11, 553-566.

Ulaby, F., Moore, R. and Fung, A. (1982): Microwave Remote Sensing: Active and Passive, Vol. II - Radar Remote Sensing and Surface Scattering and Emission Theory. Addison-Wesley, Advanced Book Program, Reading, Massachusetts, 1982, 609 pp.

Wingham, D.J., Shepherd, A., Muir, A. and Marshall, G.J. (2006): Mass Balance of the Antarctic ice sheet. Philosophical Transactions of the Royal Society A, 364(1844), 1627-1635.

Abbreviations

2D	Two dimensional
ASTER	Advanced Spaceborne Thermal Emission and Reflection radiometer
CRDP	Climate Reseach Data Package
CSV	Comma Separated Value
DEM	Digital Elevation Model
ECV	Essential Climate Variable
ESA	European Space Agency
ESRI	Environmental Systems Research Institute
FCDR	Fundamental Climate Data Record
GLAS	Geoscience Laser Altimeter System
GLIMS	Global Land Ice Measurements from Space
ICESat	Ice, Cloud, and Elevation Satellite
ID	IDentification number
IPCC	Intergovernmental Panel on Climate Change
PSD	Product Specifications Document
PUG	Product User Guide
PVASR	Product Validation and Algorithm Selection Report
RGI	Randolph Glacier Inventory
RMSE	Root Mean Square Error
SAR	Synthetic Aperture Radar
SOW	Statement of Work
SPOT	System Pour l'Observation de la Terre
SRTM	Shuttle Radar Topography Mission
TM	Thematic Mapper
UTM	Universal Transverse Mercator
WGI	World Glacier Inventory
WGMS	World Glacier Monitoring Service
WGS84	World Geodetic System with 1984 Datum